

**Particle detector calibration and performance for Horizon-T cosmic
rays experiment**

by

Murat Yessenov

A Thesis Submitted to the Faculty of the

DEPARTMENT OF PHYSICS

In Partial Fulfillment of the Requirements

For the Degree of

BACHELOR OF SCIENCE

In the School of Science and Technology

NAZARBAYEV UNIVERSITY

2017

NAZARBAYEV UNIVERSITY SCHOOL OF SCIENCE AND TECHNOLOGY

As members of the Thesis Committee, we certify that we have read the thesis prepared by Murat Yessenov entitled

PARTICLE DETECTOR CALIBRATION AND PERFORMANCE FOR HORIZON-T COSMIC RAYS EXPERIMENT

and recommend that it be accepted as fulfilling the thesis requirement for the Degree of Bachelor of Science.



Date: April 24, 2017

Dmitriy Beznosko



Date: April 24, 2017

Vassilios Kovanis

Final approval and acceptance of this thesis is contingent upon the candidate's submission of the final copies of the thesis to the Department of Physics.

I hereby certify that I have read this thesis prepared under my direction and recommend that it be accepted as fulfilling the thesis requirement.



Date: April 24, 2017

Thesis Director: Dmitriy Beznosko

Abstract

Horizon-T, a modern Extensive Air Showers (EAS) detector system, is constructed at Tien Shan high-altitude Science Station of Lebedev Physical Institute of the Russian Academy of Sciences at approximately 3340 meters above the sea level in order to study cosmic rays in energy range above 10^{16} eV coming from zenith angles $0^{\circ} - 85^{\circ}$. The detector includes eight charged particle detection points and a Vavilov-Cherenkov radiation detector. Each detection point includes a Scintillator Detector (SD) and a Glass Detector (GD) (near periphery only) connected to the Data Acquisition system via cables. The calibrations of the time delay for each cable and the signal attenuation, calibrations of SD and GD response to minimally ionizing particle passage have been completed as well as the detector response uniformity for SD. The calibration process and the results, presented in this thesis. These results were further used to tune the SD/GD simulation in order to obtain the GD response uniformity.

Due to large variation of particle density in EAS, a response linearity of each detector needs to be assessed. The number of photon in a photo multiplier tube (PMT) pulse allows inferring the deviation from linearity in each case. In order to obtain an approximate photon count of a pulse, a single photo-electron response pulse calibration for the R7723 PMT was conducted using low-level light pulse. Non-linearity measurements of PMT were conducted using the same setup. PMT signals were chosen such that their widths are comparable with the real data. Results included in this work show that the PMT signal is mostly linear and nonlinearity starts only at the upper end of ADC range.

Table of Contents

Abstract	3
Table of Contents	4
List of figures	5
List of tables	6
1. Horizon-T detector system introduction	7
1.1. System description	7
1.2. Individual detector design	7
1.3. DAQ and data analysis	8
2. Light yield measurement for SD and GD	10
2.1. MIP measurement.....	10
2.2. SD detector response uniformity	11
3. PMT Calibration	12
3.1. PMT PE calibration	12
3.2. PMT non-linearity	13
4. Simulation of GD and SD.....	16
5. Conclusion	16

List of figures

Figure 1: Horizon-T detector: Cherenkov radiation detector (left) and locations of charged particles detection points (right). Adopted from [1].....	7
Figure 2: SD detector	8
Figure 3: Example of a typical inverted PMT pulse (left) and its normalized cumulative distribution (right)	9
Figure 4: MIP calibration setup schematic for SD/GD.....	10
Figure 5: SD detector response to MIP signal	11
Figure 6: SD Detector Response Uniformity.....	12
Figure 7 : R7723 PMT single PE response pulse area at 1700V	13
Figure 8: Single PE pulse area vs. bias voltage for R7723 PMT.....	13
Figure 9: Schematic of PMT linearity measurement experiment	14
Figure 10: PIN signal area vs PMT signal area	14
Figure 11: PMT and PIN diode pulse at point 3	15

List of tables

Table 1: Coordinates of detection points. [8].....9

Table 2: Deviation of points from linearity 15

1. Horizon-T detector system introduction

1.1. System description

“Horizon-T” (HT) [1] is a recently completed detector system of a new design located at Tien Shan high-altitude Science Station (TSHASS) at approximately 3340 meters above the sea level. The TSHASS was established in 1958 as a station devoted to studying the nuclear reactions and searching for new particles in cosmic rays in a wide energy range from the galactic and extra-galactic sources. Since then, the station personnel has accumulated a vast amount of knowledge and experience, and has participated in a large number of different ground-breaking experiments over the course of years.



Figure 1: Horizon-T detector: Cherenkov radiation detector (left) and locations of charged particles detection points (right). Adopted from [1]

The current HT system consists of the Vavilov - Cherenkov radiation detector (VCD) (**Error! Reference source not found.**, left) and eight working charged particles detection points (**Error! Reference source not found.**, right) that are separated up to 500 m distance from the center point. System can measure time characteristics of the Extensive Air Showers (EAS) and record signal shapes with time resolution better than 10 ns. It was constructed to register EAS in the energy range above 10^{16} eV coming from a wide range of zenith. The time resolution and signal shape analysis capabilities of the detection points are used to study EAS development in the atmosphere. The EAS development is a process that can be studied by using spatial and temporal charged particles distribution at different distances from the EAS axis, thus a extended network of detection points is required. For the time part, a signal shape must be recorded and analyzed at each point with time resolution on the order of ns. [1]

1.2. Individual detector design

The detection points 1, 4, 5, 6 and 7 are called near periphery detectors. Each of these detection points has one scintillator detector (SD) and one glass detector (GD) [2] [3]. Both types of detector have a pyramid shape with height equal to the side. Each SD is based on polystyrene square-shaped cast scintillator that has 1 m^2 area and is 5 cm thick [4]. Each GD is based on 50 cm x 50 cm x 3 cm optical glass that is painted white with TiO_2 at the bottom side [5]. Both have the photo multiplying tube (PMT) above the scintillator/glass center. All near detectors use Hamamatsu [6] R7723 PMT assembly. Only the near periphery is equipped with GD: the fast pulse they produce gets widened by the longer cable thus diminishing the usefulness of the GL. Center temporarily has a second GL with a Hamamatsu H6527 PMT and its calibration is also included in the table.



Figure 2: SD detector

The VCD is located next to detection point 1. It consists of three parabolic mirrors of 150 cm diameter and focal length of 65 cm. They are mounted on the rotating support allowing detection in zenith angle range of 0° - 80° and in azimuthal angle range of 0° - 360° . PMT-49B (FEU49B) that is 15cm in diameter is located in the focal point of each mirror. The field of view of each mirror + PMT is $\sim 13^\circ$ from the geographical regions studied for the astroclimate, eastern Tien-Shan is well suited for Vavilov - Cerenkov radiation measurements [7] since for the most of the year there is a Rayleigh - type atmosphere when there is no aerosol present.

1.3. DAQ and data analysis

HT data acquisition system (DAQ) uses three CAEN [9] DT5730 flash analog-to-digital converters (ADC) with synchronization and self-trigger using the SD signals. [10] They receive two signals from each detection point: one from horizontal SD; one is the sum of signals from two vertical SD. Each detection point connected with DAQ via the calibrated [11] coaxial cables RK 75-7-316F-C SUPER produced by SpetsKabel [12]. The DAQ is self-triggered when signal comes from detection points 4 and 7 or 5 and 6 at the same time, meaning that EAS disk passed through

Horizon-T. This relaxed hardware trigger allows keeping a larger data sample for further offline analysis. Typical offline trigger that is applied later requires a signal at least from any four detection points. [13]

Table 1: Coordinates of detection points. [8]

Station #	X, m	Y, m	Z, m	R, m
1	0	0	0	0
2	-445.9	-85.6	2.8	454.1
3	384.9	79.5	36.1	394.7
4	-55.0	-94.0	31.1	113.3
5	-142.4	36.9	-12.6	147.6
6	151.2	-17.9	31.3	155.4
7	88.6	178.4	-39.0	203.0
8	221.3	262.0	160.7	378.7

A pulse from the MIP (minimally ionizing particle) is used for characterization of each detector. For analysis purposes, the pulse front and total duration are defined as following: the *pulse front* is between 0.1 and 0.5 of the total area under the pulse (e.g. of the pulse cumulative distribution, CDF) and the *total duration* is between the level 0.1 and level 0.9 of the pulse CDF. The example of a PMT pulse (inverted) and its normalized cumulative distribution are shown in Figure 3 (left) and in Figure 3 (right) respectively. [13]

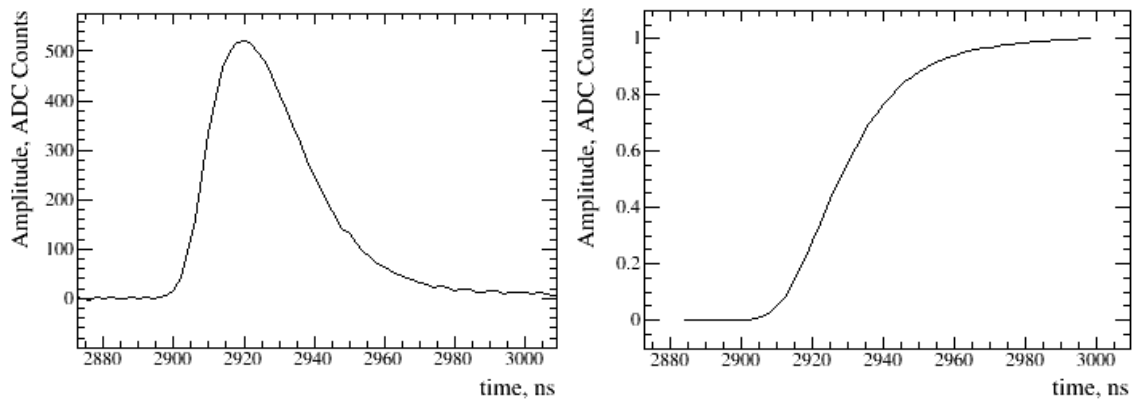


Figure 3: Example of a typical inverted PMT pulse (left) and its normalized cumulative distribution (right)

The pulse front for the R7723 PMT with scintillator is measured 7.16 ± 0.40 ns and the total duration is 21.6 ± 1.48 ns (here uncertainties are not measurement errors but a statistical spread between detection of numerous MIPs). The pulse front and the total duration for the FEU49B are 15.71 ± 0.47 ns and 38.92 ± 1.40 ns respectively.

In order to further increase the time resolution and to decouple the PMT+geometry and scintillator contributions in pulse shaping, the glass-based detector with R7723 has been constructed. The Vavilov-Cherenkov light from the charged particles in the glass is very fast compared to the PMT response time spread (~ 1.5 ns) and is on the order of ~ 0.1 ns. The pulse front for the R7723 PMT with glass is 2.17 ± 0.13 ns (with 18 m cable and including the detector geometry effects) and the total duration is 5.10 ± 0.67 . These pulse characteristics agree to the technical characteristics of the PMT. Comparison of the results obtained using the scintillator and glass indicates that the scintillator contribution to the average pulse front duration about 5 ns, and its contribution to the total duration is about 15 ns. Because of its superior time resolution, the glass detector has been installed at the detection points 1, and 4 to 7. [13]

2. Light yield measurement for SD and GD

2.1. MIP measurement

The response of each SD and GD to minimally ionizing particle (MIP) is calibrated in double coincidence setup using a secondary trigger comprised of MELTZ [14] FEU49 and a 15 cm diameter scintillator that is placed under each detector center during calibration process. Double-coincidence schema is used, facilitated by 14bit CAEN DT5730 flash ADC. The setup schematic is shown in Figure 4.



Figure 4: MIP calibration setup schematic for SD/GD.

The resulting calibration gives the area of a single MIP signal as well as the width of the MIP signal pulse from each SD/GD. The uncertainty, associated with the size of the integration window is included in the total error. The waveform recorded by the ADC consist of 5110 data points digitized every 2 ns each, for the total of $10.22 \mu\text{s}$. The full digitization range of 2^{14} bins corresponds to 2 V. The areas are given in the custom units of ADC counts \cdot ns. [15]

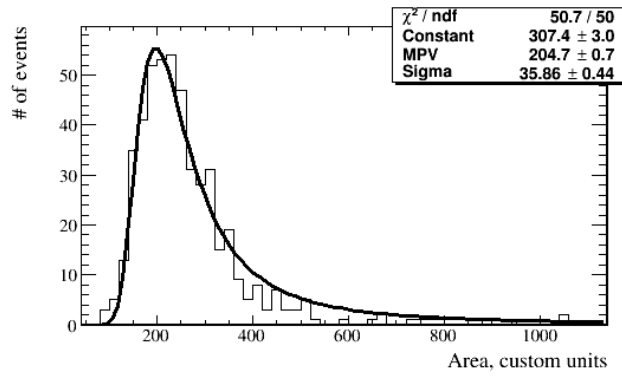


Figure 5: SD detector response to MIP signal

As with any calibration, where the detector that is being calibrated is also part of the triggering, there is also a question of the threshold enforced on the detector that is being calibrated. Here we use the threshold as low as possible but still above a pedestal value. For that, a threshold of a few mV is used first and the data is taken with a pedestal clearly visible. Then the data is retaken with the threshold value right above the pedestal value since for all detectors there is a clear separation between the pedestal and the lowest MIP signal. The Landau curve fit gives the most probable value (MPV) used for the calibration. Care is taken to make sure that chosen threshold value doesn't affect the resulting calibration value (e.g. any possible shift in area MPV is much smaller than the associated uncertainty). The example fit of a MIP signal area for the SD from detection point 1 (Center) is shown in Figure 5. Fit is done using ROOT [16] package PyROOT, areas are found using trapezoidal method [17]. A fit to a Landau distribution is used since the (relatively) thin target is used.

Recent results of the MIP calibration are shown in [8]. All cable effects are included in the calibration; MPV (top value) and σ (bottom value) with corresponding fit uncertainties are listed.

In order to compare with the detector simulation, the single photo-electron (PE) area calibration for R7723 PMT is done (detailed explanation of calibration is in *PMT PE calibration* section). PE number for each scintillator and glass detector is calculated using MIP pulse area and single PE PMT response area of corresponding detector. Signal losses in each cable [11] and presence of impedance matching resistor are also taken into account. As a result, average PE number obtained for SD is 45.2 ± 4.5 photons, and PE number for GD is 1.8 ± 0.6 photons. A specific PE per MIP value for the SD used as a reference for simulation was 37.1 ± 4.5 photons.

2.2. SD detector response uniformity

The MIP signal calibration is done at the center of SD or GD, however, particles arrive randomly. Thus, a number of particles will be distributed uniformly across the detector area, and we

need to measure the non-uniformity of detector response in order to estimate the charged particle flux through each SD.

In order to measure the non-uniformity, each SD is scanned across using ^{60}Co radioactive source along the lines $x = 20$ cm, $x = 80$ cm and two diagonals. PMT dark current (e.g. current measured without rad. source) is subtracted. Data is normalized to maximal value for uniformity comparison across different lines. The I/I_{max} vs distance is shown in Figure 6. The size of error bars is due to the low intensity of the rad. source that was available.

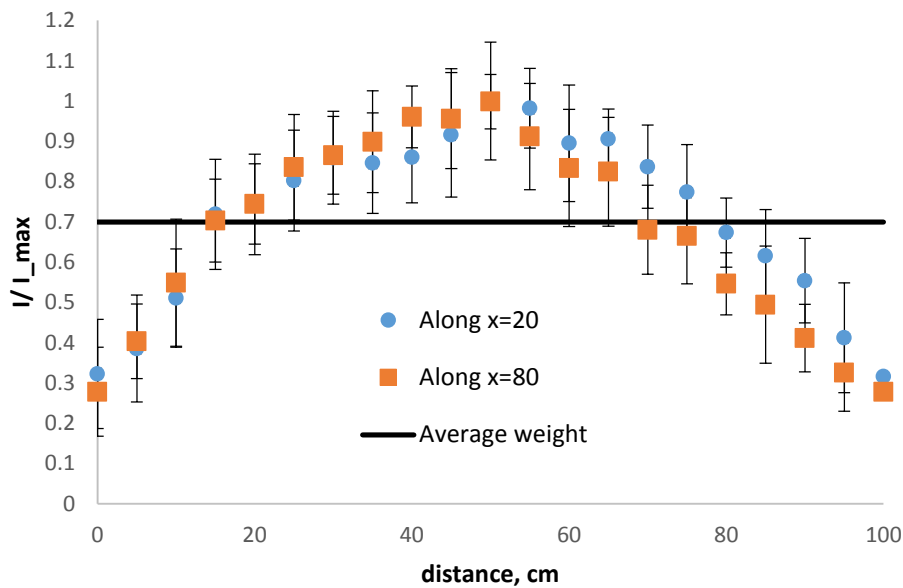


Figure 6: SD Detector Response Uniformity.

Light yield of scintillator itself is uniform across its volume; the rest is the effect of the detector shape (e.g. geometry). Based on that, the normalized detector response data is scaled by an average value weight. The average weight value is obtained by finding a line such as the area under it equals to the area under the data points. Average weight value for several SDs is 0.7 ± 0.1 .

3. PMT Calibration

3.1. PMT PE calibration

In order to obtain an approximate photon count for each MIP calibration to be used for tuning of detectors simulation we do the PE response pulse area calibration for the R7723 PMT. For that, low light LED (light emitting diode) pulse is fed to PMT that is connected to DAQ via short cable (<1m). Trigger is provided by the LED power source. Since signal is baseline subtracted, the

pedestal is very low and is removed from later fit. Care is taken to ensure that pedestal has about 80% of all events in order for single photon detection assurance. Figure 7 shows the pulse area of PMT single PE response at 1700V with pedestal subtracted. PMT is calibrated at the different bias voltages to match different detectors.

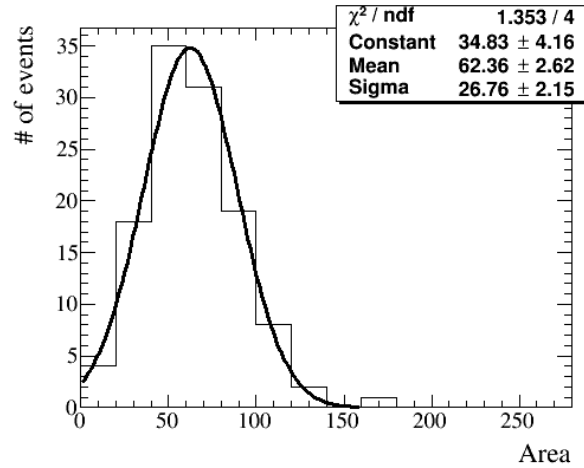


Figure 7 : R7723 PMT single PE response pulse area at 1700V

In Figure 8, the single PE area vs biasing voltage is shown. For the R7723 PMT, we can see that it is linear for a very wide range of biases, with 2000V being recommended maximum and pulses becoming too close to noise below 1300V for accurate calibration.

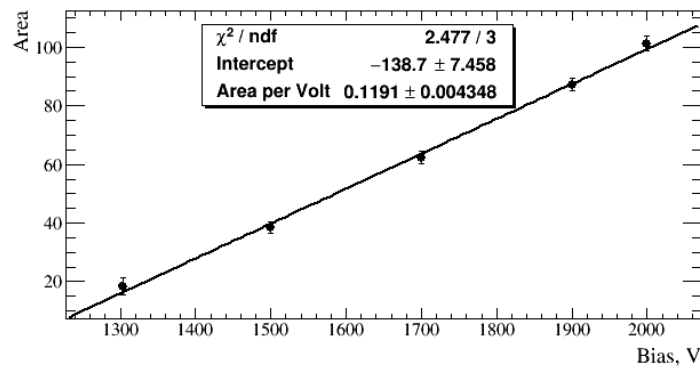


Figure 8: Single PE pulse area vs. bias voltage for R7723 PMT

Eventually, PMT single PE calibration is needed to calculate number of incident photons in PMT pulse signal during detector operations.

3.2. PMT non-linearity

The PMT response saturates for large input signals. In order to interpret cosmic rays data correctly and obtain the charged particles density distribution, non-linearity measurements for R7723 PMT were conducted in the range of output voltages that slightly exceeds the ADC range. For this measurement, setup schematic is shown in Figure 9.

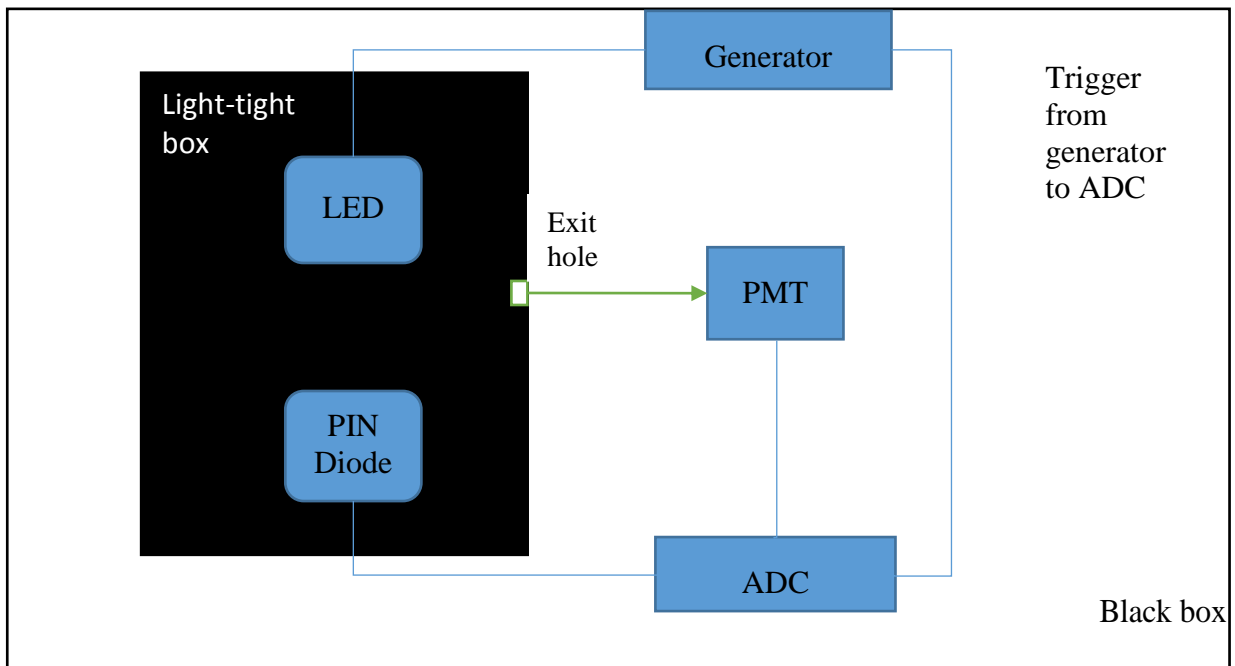


Figure 9: Schematic of PMT linearity measurement experiment

Initially, PMT and Hamamatsu S3883Si PIN diode responses were measured for small signals with several photons detected, where PMT response is guaranteed to be linear. PIN diode is used because its response is known to be linear up to its detection limit (on the order of 10^{10} photons). Intensity of incident light is gradually increased and signal from PMT and PIN diode are measured. The PIN diode signal area vs PMT signal area is plotted and shown in Figure 10.

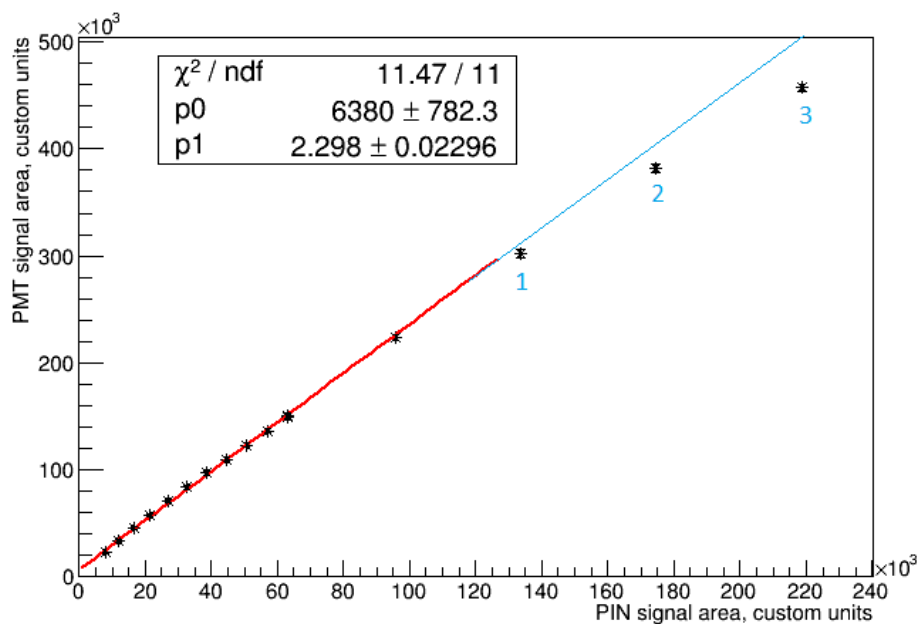


Figure 10: PIN signal area vs PMT signal area

It can be seen from the graph above that starting from point labeled as 1, PMT response is nonlinear. Nonlinearity could be estimated by deviation of the signal from the fit line. Deviations for three points are shown in Table 2.

Table 2: Deviation of points from linearity

	Deviation, %
Point 1	3.7 ± 0.3
Point 2	6.6 ± 0.2
Point 3	11.3 ± 0.2

Deviation of signal corresponding to point 3 is considerably larger than two previous points, and so this point is considered in more details. From the shapes of PMT pulse and PIN diode pulse shown in Figure 11, one can see that PMT signal is cut; this means ADC saturation is reached. So, PMT signal starts to be nonlinear with deviation $\sim 7\%$ near the ADC upper range limit.

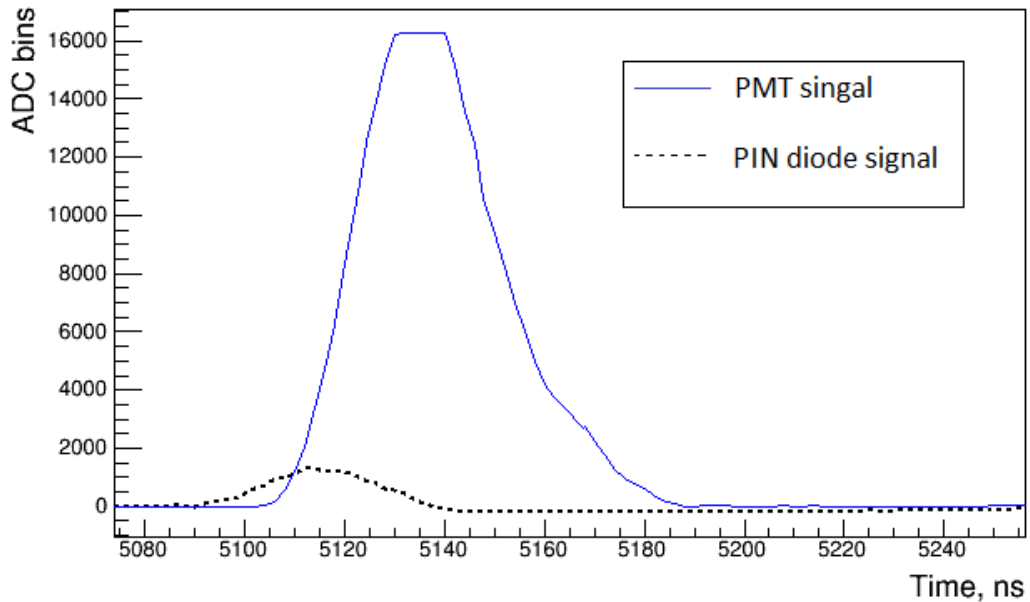


Figure 11: PMT and PIN diode pulse at point 3

4. Simulation of GD and SD

As it was mentioned before, light yield per particle for SD and GD were obtained and uniformity of SD was measured. These values were used to set parameters of detector simulation. Experimental value of average weight (measure of uniformity) for SD is 0.7 ± 0.1 , while we find it to be 0.70 ± 0.11 from simulation. So, there is close match. The same parameters were used to make simulation of GD and obtained value of average weight for GD is 0.74 ± 0.07 . So, according to our simulation, GD response is more uniform when compared to SD response.

5. Conclusion

Horizon-T is a modern detector system that measures time characteristics of the EAS and record signal shapes with time resolution better than 10 ns. Such high resolution needs accurate calibration of all components of the experiment. Light yield of SD and GD is assessed. For that, the calibration of SD and GD response using single MIP signal is done, as well as SD detector response uniformity is measured, and attenuation and signal loss in cables were taken into account. These results were further used to set parameters for the SD and GD simulation in order to obtain GD response uniformity.

In order to obtain an approximate photon count for a pulse, PE response pulse calibration for the R7723 PMT was conducted. In addition, a linearity and saturation of each detector is assessed by measurement of PMT and PIN diode response for different number of incident photons. Results show that the PMT signal linearity is conserved within most part of the operational range and starts reach saturation close to the end. Deviation from linearity is measured. The details of all calibrations and numerical values of measurements are provided in this thesis.

References

- [1] D. Beznosko et al., "Horizon-T Extensive Air Showers detector system operations and performance," in *PoS(ICHEP2016)784, proceedings of ICHEP2016*, Chicago, 2016.
- [2] D. Beznosko, G. Blazey, A. Dyshkant, V. Rykalin, J. Schellpffer and V. Zutshi, "Modular Design for Narrow Scintillating Cells with MRS Photodiodes in Strong Magnetic Field for ILC Detector," *Nuclear Instruments and Methods in Physics Research Section A*, Volume 564, pages 178-184, 2006/8/1.
- [3] A. Dyshkant, D. Beznosko, G. Blazey, E. Fisk, E. Hahn, V. Rykalin, M. Wayne and V. Zutshi, "SCINTILLATION DETECTORS-Quality Control Studies of Wavelength Shifting Fibers for a Scintillator-Based Tail Catcher Muon Tracker for Linear Collider Prototype Detector," *IEEE Transactions on Nuclear Science*, volume 53, issue 6, page 3944, 2006.
- [4] Adil Baitenov, Alexander Iakovlev, Dmitriy Beznosko, "Technical manual: a survey of scintillating medium for high-energy particle detection," *arXiv:1601.00086*, 2016/1/1.
- [5] M. Yessenov, A. Duspayev, T. Beremkulov, D. Beznosko, A. Iakovlev, M.I. Vildanova, K. Yelshibekov, V.V. Zhukov, "Glass-based charged particle detector performance for Horizon-T EAS detector system," *arxiv:1703.07919*, 03/2017.
- [6] Hamamatsu Corporation, 314-5, Shimokanzo, Toyooka-village, Iwatagun, Shizuoka-ken, 438-0193 Japan. <http://www.hamamatsu.com>.
- [7] T. B. Omarov, A. K. Kurchakov, B. I. Demchenko, U. M. Zavarzin., "Astroclimate of high altitude plateau Assi-Turgen," *Almaty: Science*, p. 59, 1982.
- [8] D. Beznosko, T. Beremkulov, A. Iakovlev, A. Duspayev, M. I. Vildanova, T. Uakhitov, K. Yelshibekov, M. Yessenov, V.V. Zhukov, "Horizon-T Experiment Calibrations – MIP Signal from Scintillator and Glass Detectors," *arxiv:1703.07559*, 3/2017.
- [9] CAEN S.p.A. Via della Vetraila, 11, 55049 Viareggio Lucca, Italy. <http://caen.it>.
- [10] Duspayev, A., R. U. Beisembaev, T. Beremkulov, D. Beznosko, A. Iakovlev, K. Yelshibekov, M. Yessenov, V. Zhukov, "Simulation, design and testing of the HT-KZ Ultra-high energy cosmic rays detector system," *Proceedings of ICHEP2016*, vol. PoS(ICHEP2016)721, 2016.

- [11] D Beznosko, T Beremkulov, A Iakovlev, Z Makhataeva, M I Vildanova, K Yelshibekov, VV Zhukov, "Horizon-T Experiment Calibrations-Cables," *arXiv:1608.04312*, 8/2016.
- [12] SpetsKabel Inc., 6/1-5 Birusinka St., Moscow, Russia. <http://www.spetskabel.ru/>.
- [13] RU Beisembaev, EA Beisembaeva, OD Dalkarov, VA Ryabov, AV Stepanov, NG Vildanov, MI Vildanova, VV Zhukov, KA Baigarin, D Beznosko, TX Sadykov, NS Suleymenov, "The 'Horizon-T' Experiment: Extensive Air Showers Detection," *arXiv:1605.05179* [physics.ins-det], May 17 2016.
- [14] MELZ-FEU, 4922-y pr-d, 4c5, Zelenograd, g. Moskva, Russia, 124482 (<http://www.melz-feu.ru>).
- [15] D. Beznosko, T. Beremkulov, A. Duspayev, A. Iakovlev, "Random Number Hardware Generator Using Geiger-Mode Avalanche Photo Detector," in *PoS(PhotoDet2015)049*, in *proceedings to PhotoDet2015*, Moscow, 2015.
- [16] R. Brun, F. Rademakers, "ROOT: An object oriented data analysis framework," *Nucl. Instrum. Meth. A*, vol. 389, p. 81–86, 1997.
- [17] "numpy.trapz," [Online]. Available: <http://docs.scipy.org/doc/numpy-1.10.1/reference/generated/numpy.trapz.html>.